Design of stainless steel structural systems by GMNIA with strain limits

H.U. Chan
F. Walport, D.A. Nethercot, L. Gardner
Department of Civil and Environmental Engineering, Imperial College London

Imperial College London

INTRODUCTION

- Stainless steel is a high value material characterised by a rounded stress-strain relationship with early deviation from linear elastic behaviour and significant strain hardening.
- Current design standards for stainless steel structures were developed largely in line with those for carbon steel structures, which is based on an idealised bilinear (elastic, perfectly plastic) material response → inefficient structural design.
- A new design framework utilising advanced analysis techniques and computationally efficient beam finite elements (FE) is presented.

NEW DESIGN FRAMEWORK

Beam FE GMNIA (Geometrically and Materially Nonlinear Analysis with Imperfections) + **Strain limits** defined using Continuous Strength Method (CSM) = **Ultimate resistance**

Beam FE GMNIA captures:
- Strain hardening
- Force and moment redistribution
- Moment gradient effect on member instability

Beam FE GMNIA captures (controls the extents of):
- Local buckling
- Member buckling
- Frame buckling
- Material yielding

Strain limits captures:
- Local buckling

Strain limits allows for:
- Moment gradient effect on local instability
- Influence of shear

Ultimate resistance → safety factors → **Design resistance**

- Traditional step-wise cross-section checks accounting for local buckling replaced by the application of strain limits, which is dependent on cross-section slenderness $\bar{\lambda}_p$.
- Failure is defined as first to occur of peak load or strain limit reached in analysis.

CSM strain limit ε_{csm} calculated using:

$$\frac{\varepsilon_{csm}}{\varepsilon_y} = \frac{0.25}{\bar{\lambda}_p^{3.6}} + \frac{0.002}{\varepsilon_y} \quad \text{but} \quad \frac{\varepsilon_{csm}}{\varepsilon_y} \leq 15 \quad \text{for } \bar{\lambda}_p \leq 0.68$$

$$\frac{\varepsilon_{csm}}{\varepsilon_y} = \left(1 - \frac{0.222}{\bar{\lambda}_p^{1.05}}\right)\frac{1}{\bar{\lambda}_p^{1.05}} + \frac{0.002(\sigma/f_y)^n}{\varepsilon_y} \quad \text{for } 0.68 < \bar{\lambda}_p \leq 1.0$$

RESULTS

- Ultimate capacity predictions α_{ult} obtained from the presented design method and the traditional stainless steel design procedures according to EN 1993-1-4 compared against benchmark ultimate loads determined using shell FE models α_{shell}:

2-span continuous beam

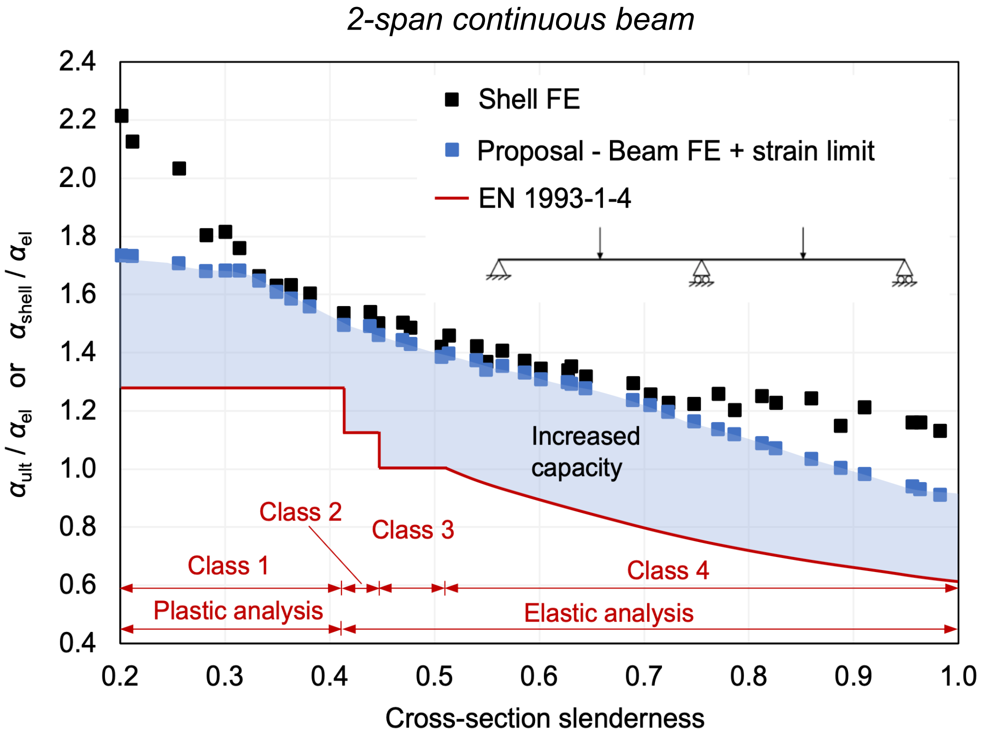

Single storey portal frame

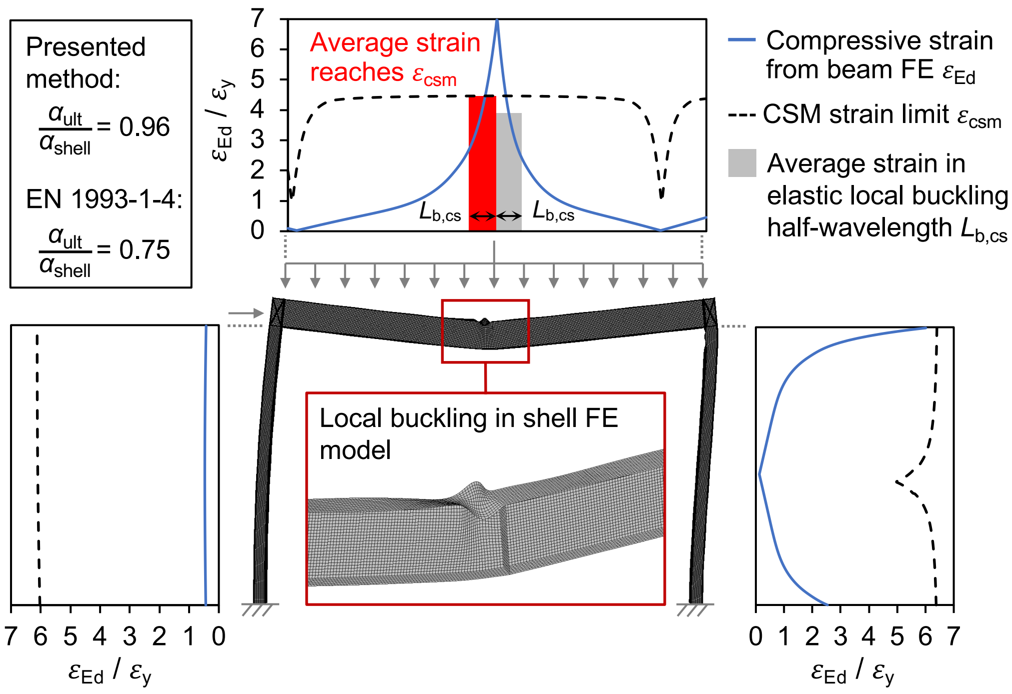

- Presented method gives close and generally safe-sided capacity predictions to benchmark results and accurately captures failure mechanism.
- The overly conservative EN 1993-1-4 predictions confirms the significance of appropriate allowances in the proposed method for the beneficial effects of plastic redistribution, strain hardening and local moment gradient.

CONCLUSIONS

- Challenges presented by nonlinear stress-strain response of stainless steel are overcome in the presented design method by employing advanced analysis technique (GMNIA) with beam finite elements and strain limits.
- Presented design method shown able to provide more accurate and consistent capacity predictions than EN 1993-1-4.
- Due to be included in AISC 370 and prEN 1993-1-14, offering a step change in efficiency for the future direction of structural stainless steel design.

Walport, F., Chan, H.U., Gardner, L. & Nethercot, D.A. (2023). Design of stainless steel structural systems by GMNIA with strain limits, Engineering Structures, 276, 115339.

Mechanical and structural behaviour of rubberised alkali-activated concrete

Mohamed Elzeadani (m.el-zeadani20@imperial.ac.uk) | Supervised by: Ahmed Elghazouli, Dan Bompa
Department of Civil and Environmental Engineering, Imperial College London, London, UK

The Institution of StructuralEngineers
Young Researchers Conference 2023
Imperial College London

1. Background

- Cement production is responsible for 5-8% of global carbon emissions.
- Alkali-activated concrete employs no cement in the mix design.
- Rubber particles from discarded end-of-life tyres are used to replace a proportion of the natural aggregates.

2. Aims and Methods

Aims:
- Develop an optimised mix design.
- Characterise the mechanical and structural behaviour.

Methods:
- Experimental testing of concrete specimens.

3. Optimised Mix Design

Fig. 1: Constituent materials

Table 1: Optimised concrete mix designs (kg/m^3)

Mix ID	Slag	Fly ash	Act.	Admix.	Sand	Gravel	Rubber	Water
R00	480	120	72	30	675	825	0	180
R30	480	120	72	30	473	578	163	180
R60	480	120	72	30	270	330	326	180

4. Mechanical Properties

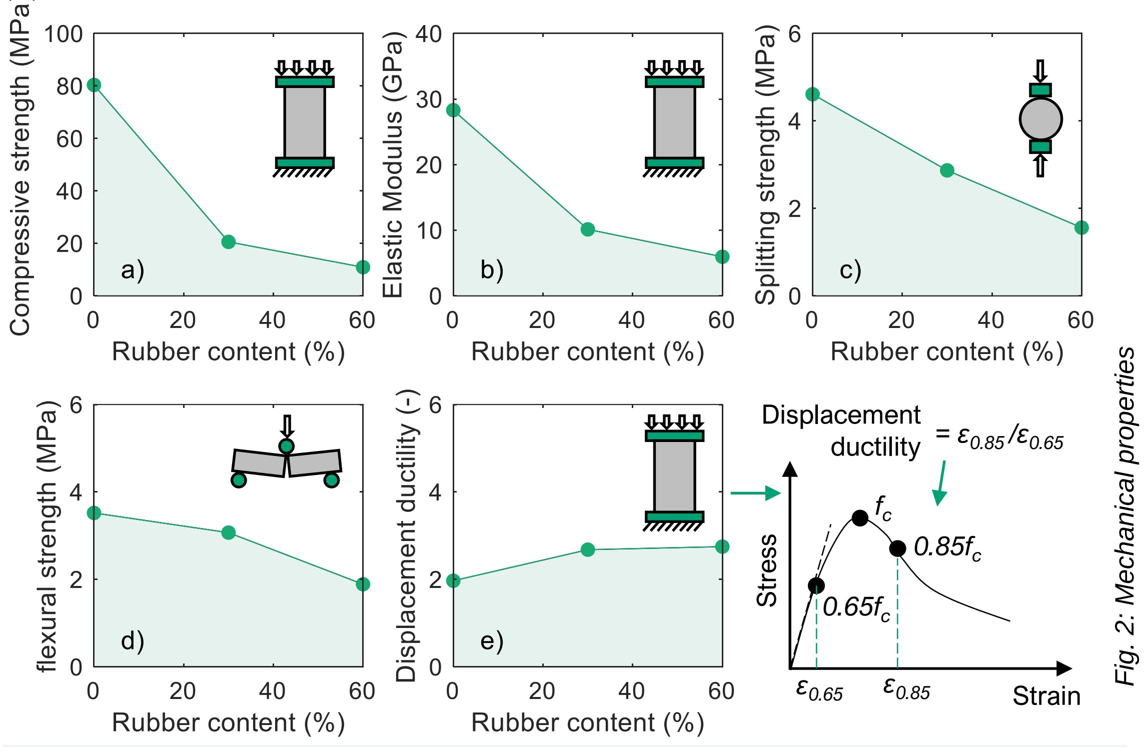

Fig. 2: Mechanical properties

5. Cyclic Response

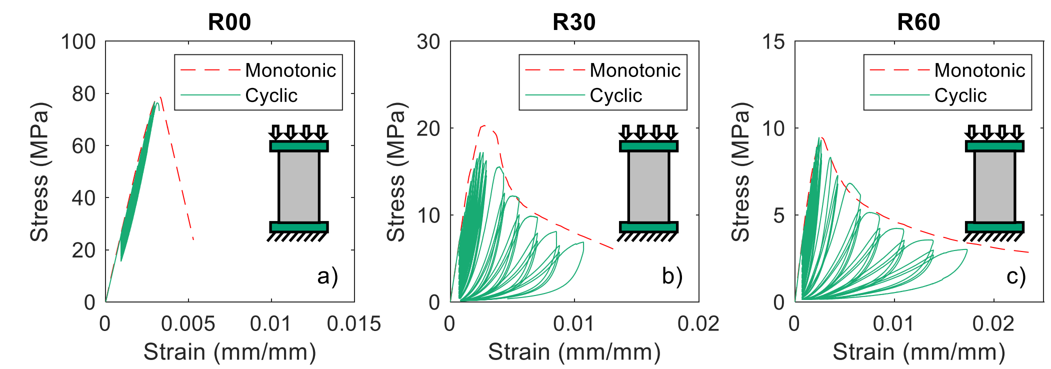

Fig. 3: Cyclic stress-strain response

6. Impact Response

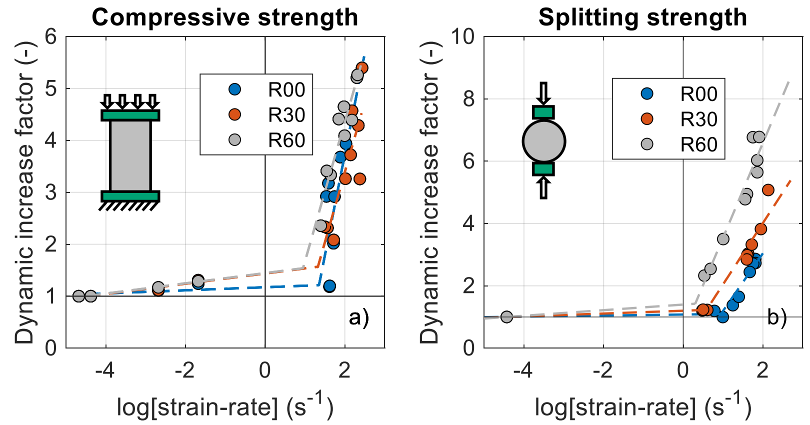

Dynamic increase factor:

$$\frac{\text{Dynamic strength}}{\text{Quasi-static strength}}$$

Fig. 4: Dynamic increase factors

7. Confined Axial Behaviour

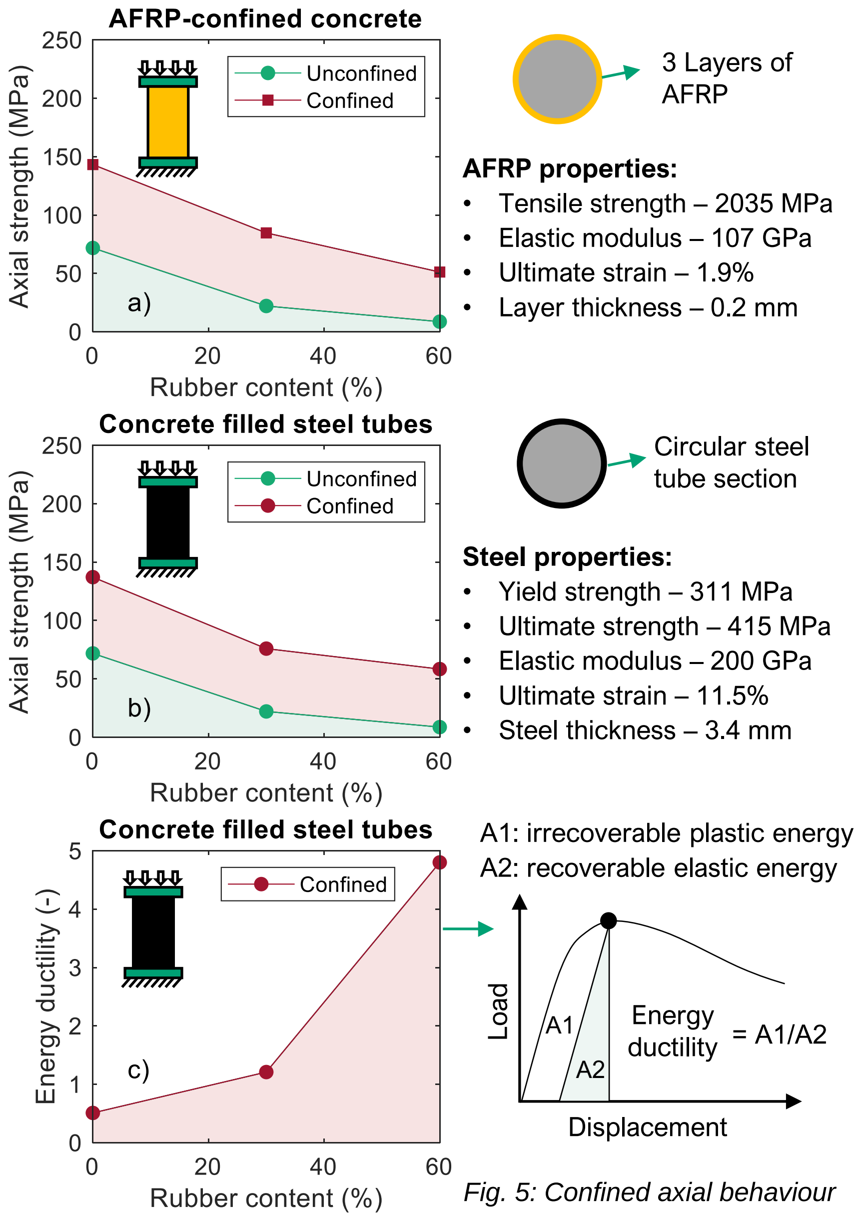

AFRP properties:
- Tensile strength – 2035 MPa
- Elastic modulus – 107 GPa
- Ultimate strain – 1.9%
- Layer thickness – 0.2 mm

Steel properties:
- Yield strength – 311 MPa
- Ultimate strength – 415 MPa
- Elastic modulus – 200 GPa
- Ultimate strain – 11.5%
- Steel thickness – 3.4 mm

Fig. 5: Confined axial behaviour

8. Conclusions

- Rubber addition significantly enhances the ductility of concrete and gives a more favourable post-peak degradation behaviour.
- Confinement of specimens can help overcome some of the challenges of rubber addition.

Acknowledgements

- The funding provided by the President's PhD Scholarship at Imperial College London is gratefully acknowledged.

PHYSICS-INFORMED NEURAL NETWORKS FOR DATA-DRIVEN DESIGN MODELS

MACHINE LEARNING FOR STRUCTURAL DESIGN WITHOUT CREATING A BLACK BOX

ADRIEN GALLET[a,*], DR ANDREW LIEW[a], PROF IMAN HAJIRASOULIHA[a] & DR DANNY SMYL[b]

Date: 2023.03.23 [a] University of Sheffield [b] University of South Alabama * Email: agallet1@sheffield.ac.uk

THE PROBLEM

The lack of real-time feedback providing accurate engineering insight on design decisions is a major hurdle for modern structural engineers [1]. By treating structural design as an inverse problem [2], one can use a learned as opposed to iterative solution approach to provide instantaneous design solutions. Such a data-driven design model can be used to design continuous beam systems.

Continuous beam with UDLs w, spans L and section-properties W_{pl}

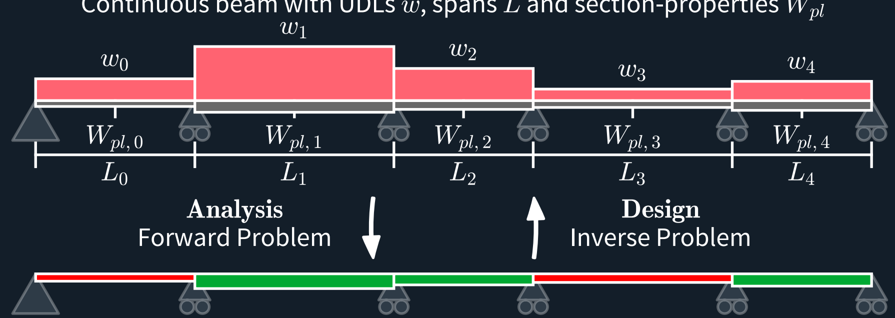

ULS structural compliance checks

WHY PINNs FOR DATA-DRIVEN DESIGN?

Typical machine learning models rely only on data-points to construct the loss-function $\boldsymbol{L}_{\text{data}}$ to minimise the error between $\boldsymbol{Y}_i$ and $\hat{\boldsymbol{Y}}_i$, the true and predicted values respectively. Such black box models cannot be easily validated.

$$\boldsymbol{L}_{\text{data}} = \frac{1}{n}\sum_{i=1}^{n}\left(\boldsymbol{Y}_i - \hat{\boldsymbol{Y}}_i\right)^2$$

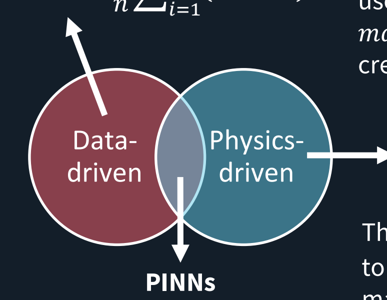

$$\boldsymbol{L}_{\text{PINN}} = \boldsymbol{L}_{\text{data}} + \boldsymbol{L}_{\text{physics}}$$

Physics informed neural networks (PINNs) [3] use proven physical relationships (e.g. $F = ma$) expressed as physics equations $\boldsymbol{P}(\boldsymbol{x})$ to create a physics-loss function $\boldsymbol{L}_{\text{physics}}$.

$$\boldsymbol{L}_{\text{physics}} = \frac{1}{n}\sum_{i=1}^{n}\left(\hat{\boldsymbol{Y}}_i - \boldsymbol{P}(\boldsymbol{x})_i\right)^2$$

The $\boldsymbol{L}_{\text{physics}}$ loss function regularises outputs to inputs, and forces the neural network to make physically realistic results. Combining data- and physics-driven losses results in the PINN's loss function $\boldsymbol{L}_{\text{PINN}}$.

HOW IT WORKS: Data-driven models need to be both generalisable and accurate/robust to achieve wide-spread usability.

1. Influence zone evaluation

To apply the PINN to any continuous beam system, the recently developed influence zone concept is implemented [4]. The influence zone $k_{\max}$ indicates the extent to which surrounding design information are relevant for the design of a beam.

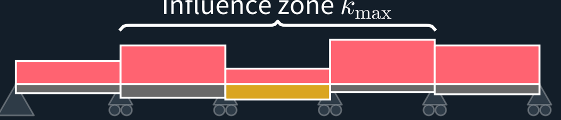

By evaluating the influence zone for design conditions that arise in steel-framed buildings, it is possible to statistically infer the maximum influence zone size to be $k_{\max} = 5$ (see figure below). A PINN whose inputs contain the information from this influence zone can be applied to any continuous beam system.

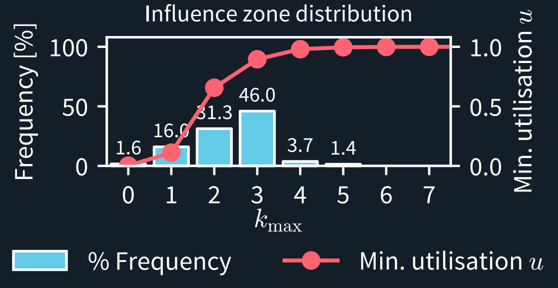

2. Physics-informed loss equations

The physics equations $\boldsymbol{P}(\boldsymbol{x})$ chosen for the PINN's $\boldsymbol{L}_{\text{physics}}$ loss function were the Timoshenko stiffness matrices. By relating the internal forces to cross-sectional properties and by providing fixed end-moment adjustments, it is possible to relate the input variables, UDL(s) ω and spans L, to the output variable(s), such as the plastic section modulus W_{pl} (see diagram on the right).

$$P(x) = W_{pl} = \left(\frac{EI}{L^3(1+\varphi)}\left(6Lu_1 + (4+\varphi)L^2\theta_1 - 6Lu_2 + (2-\varphi)L^2\right) - \frac{\omega L^2}{12}\right)\frac{1}{f_y}$$

Further $P(x)$ equations could be constructed for other output variables (I_{yy}, A_z, etc.). By extracting the remaining variables ($E, u, \theta, f_y, \varphi$) from the critical design check during data generation, the PINN is ready for training.

A simplified view of the PINN

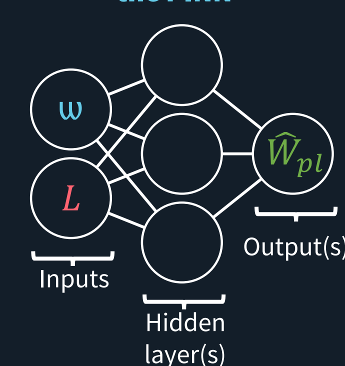

3. Data generation and preliminary results

100k different continuous beam systems was designed with varying UDLs and spans using a coupled analysis and design approach [5]. The performance of the PINN in comparison to a standard data-driven NN and a simple linear model is shown below, expressed in terms of validation accuracy (target accuracy is 10^0 = 100%).

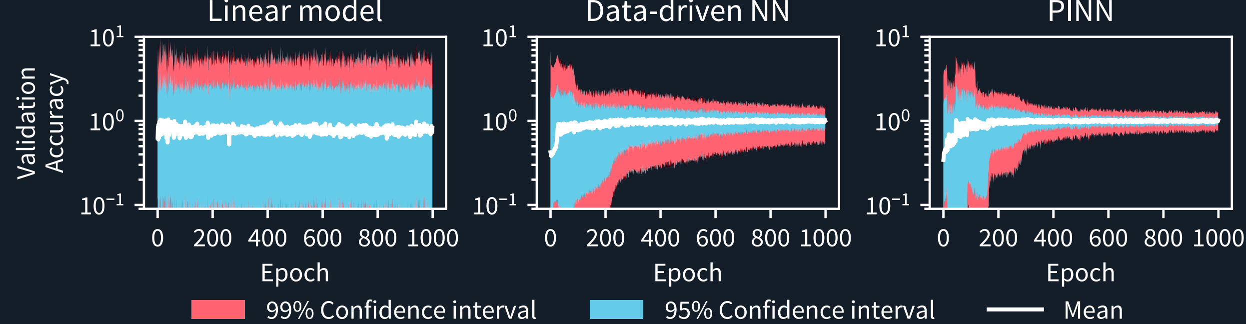

SCAN THE QR CODES!

Homepage RG Profile

University of Sheffield
USA
UKRI Engineering and Physical Sciences Research Council
RAMBØLL FONDEN

REFERENCES

[1] D. Sinclair, A. Tait, L. Carmichael, *RIBA Plan of Work Overview*, RIBA, London, 2020

[2] A. Gallet et al., Structural engineering from an inverse problems perspective, *Proceedings of the Royal Society A: Mathematical, Physical and Engineering Sciences* 478 (2257) (2022)

[3] M. Raissi et al., Physics-informed neural networks: A deep learning framework for solving forward and inverse problems involving nonlinear partial differential equations, *Journal of Computational Physics* 378 (2019) 686–707

[4] A. Gallet et al., Influence zones for continuous beam systems (2023)

[5] M. P. Saka, Z. W. Geem, Mathematical and Metaheuristic Applications in Design Optimization of Steel Frame Structures: An Extensive Review, *Mathematical Problems in Engineering* (2013)

CONCLUSIONS & FUTURE STEPS

As shown by the results, the PINN model provides better validation accuracy convergence than the other models, an indication of improved robustness. Future steps include testing out various physics equations $\boldsymbol{P}(\boldsymbol{x})$, expanding the application to 2D structures, and providing improved interpretability during inference.

2D steel frame